Enhanced Vehicle Dynamics through Constrained Model Predictive Control for In-Wheel Active Suspension Systems

Trong Tu Do*

Faculty of Mechanical-Automotive and Civil Engineering, Electric Power University, Hanoi, Vietnam

Received 25 August 2025; received in revised form 13 November 2025; accepted 14 November 2025

DOI: https://doi.org/10.46604/peti.2025.15624

Abstract

This study develops and evaluates a Model Predictive Control (MPC) strategy to enhance the dynamic performance of vehicle suspension systems subjected to stochastic road excitation. A high-fidelity simulation environment is established using a quarter-car model and a road profile conforming to ISO 8608:2016 Class B standards, with a constant vehicle speed of 60 km/h. The proposed constrained MPC algorithm, which predicts system states and optimizes control inputs over a finite horizon, is benchmarked against a conventional passive suspension. Simulation results demonstrate the MPC controller's superior efficacy in attenuating vibrations across a broad frequency range, resulting in significant improvements in both ride quality and handling stability. Key performance metrics include a 36.44% reduction in sprung mass acceleration (enhancing passenger comfort), an 18.71% reduction in unsprung mass acceleration (improving vibration isolation), and a 6.02% reduction in hub acceleration (promoting stable tire-road contact).

Keywords: model predictive control, vehicle suspension, ride comfort, vibration isolation, in-wheel active suspension systems

1. Introduction

The suspension system is a critical subsystem in modern vehicles, directly influencing ride comfort, road-holding capability, and overall safety. Traditional passive suspension systems, composed of fixed springs and damping elements, have long been the industry standard due to their simplicity and low cost. However, their inability to adapt to varying road surfaces and driving conditions results in an inherent trade-off between ride comfort and handling stability [1-3]. This trade-off becomes increasingly restrictive in the context of modern intelligent and electrified vehicles, where passenger comfort and vehicle performance must be optimized simultaneously.

To overcome these limitations, research has progressed from passive to semi-active and ultimately to Active Suspension Systems (ASS). Semi-active suspensions, which utilize controllable dampers to adjust damping forces in real time, offer improved adaptability and better trade-offs between comfort and stability. Nevertheless, because they cannot actively inject energy into the system, their effectiveness diminishes under severe driving conditions [1, 4]. In contrast, active suspensions represent a paradigm shift by enabling actuators to regulate suspension forces directly. Early investigations employed classical control approaches such as PID and Skyhook control, which achieved noticeable vibration suppression but were hindered by sensitivity to nonlinearities and parameter variations [2, 5-7]. Subsequent studies introduced more advanced strategies, including the Linear Quadratic Regulator, H_∞ control, and Sliding Mode Control, which enhanced robustness and performance. However, these methods often struggle with handling multiple conflicting objectives and explicit system constraints, both of which are critical in real-world applications [8-10].

* Corresponding author. E-mail address: tudt@epu.edu.vn

In parallel with these control developments, the rapid adoption of electric vehicles and autonomous vehicles has motivated the exploration of in-wheel active suspension systems (IW-ASS) [11-12]. In IW-ASS, both the suspension actuation and control mechanisms are integrated directly into the wheel hub. This architecture enables modularity, compact design, and potentially simpler powertrain layouts. However, it introduces unique challenges, particularly the increased unsprung mass and hub vibrations, which negatively affect ride comfort and road-holding capability [7]. These dynamics require more advanced control strategies that can balance competing objectives, such as comfort, stability, and road safety, while explicitly managing system constraints.

Among modern approaches, Model Predictive Control (MPC) has emerged as a powerful candidate for suspension applications [13-14]. MPC predicts future system states over a finite horizon and optimizes control inputs while explicitly considering constraints on states and actuators. Unlike classical controllers, MPC can anticipate upcoming road disturbances and adjust control actions proactively. Previous works have demonstrated that MPC enhances both comfort and stability compared to conventional control methods [15-19]. Recent research on IW-ASS has focused on simultaneously improving ride comfort, handling stability, energy efficiency, and vibration suppression. One direction emphasizes regenerative suspension systems, where electromagnetic actuators and advanced converters not only enhance comfort by emulating skyhook and conventional dampers but also harvest vibration energy for improved efficiency (with reported gains up to 52% in comfort and measurable energy recovery across road classes) [20-22].

Another line of work develops hierarchical control strategies for four in-wheel drive EVs, combining lateral stability controllers and torque distribution mechanisms to maintain yaw and sideslip stability under critical driving conditions, demonstrating superior handling performance compared to traditional strategies. Additionally, hybrid vibration suppression and suspension optimization methods have been proposed, where linear quadratic regulators and finite-frequency controllers jointly reduce in-wheel motor vibration and improve ride comfort, constrained by suspension workspace and road-holding ability [23-24]. Techniques such as fuzzy non-fragile finite-frequency H_∞ control, hybrid MPC, and multi-objective optimization have been developed to suppress electromechanical coupling effects, enhance suspension dynamics, and improve braking and torque performance, while novel structural designs and commutation methods further mitigate unbalanced forces and acoustic noise.

Additionally, co-design frameworks integrating event-triggered communication and active suspension control highlight the trend toward holistic solutions that simultaneously improve vehicle comfort, safety, energy efficiency, and real-time performance in IWM-driven electric vehicles [10, 25-26]. Huang et al. proposed a sine-resistance network motion planning approach for autonomous electric vehicles, emphasizing smooth and collision-free trajectories in dynamic environments. Meanwhile, adaptive bioinspired preview suspension controllers incorporating constrained velocity planning have been suggested to improve ride comfort for autonomous vehicles by combining preview information with biologically inspired dynamics [27-28]. Additionally, approximation-free prespecified-time bionic reliable controllers have been developed to provide fault-tolerant, energy-efficient suspension control with guaranteed transient performance [29]. While bioinspired and preview-based controllers target robustness and reduced energy consumption, the constrained MPC presented here focuses on predictive multi-objective optimization under explicit actuator and deflection limits for IW-ASS configurations.

Despite these promising outcomes, the majority of existing MPC studies have focused on conventional suspension architectures [3]. Comprehensive investigations of MPC applied specifically to IW-ASS remain limited, particularly under standardized road disturbance models such as those defined by ISO 8608. Moreover, there is a lack of systematic comparative studies between passive and MPC-controlled IW-ASS, which are crucial for quantifying the benefits and limitations of MPC in the context of electric vehicle suspension systems [1, 27].

Motivated by these research gaps, this paper develops a three-mass quarter-car IW-ASS model comprising sprung mass, unsprung mass, and hub dynamics. The proposed MPC controller is designed with explicit actuator force constraints and

optimized weighting factors to minimize body acceleration, unsprung mass vibration, and hub oscillations. Road disturbances are modeled according to ISO 8608 Class B standards to ensure realistic testing conditions. Comparative simulations between passive and MPC-controlled IW-ASS are conducted to evaluate ride comfort and vibration suppression performance. The contributions of this paper are threefold:

(1) Development of a detailed three-mass IW-ASS model that incorporates sprung mass, unsprung mass, and wheel hub dynamics.
(2) Design and implementation of an MPC controller with explicit force constraints and multi-objective optimization tailored to IW-ASS.
(3) A systematic comparative analysis between passive and MPC-controlled IW-ASS under ISO 8608 Class B road excitations, providing a quantitative evaluation based on standard deviation reduction of body acceleration, unsprung vibration, and hub oscillations.

The remainder of this paper is organized as follows. Section 2 presents the mathematical modeling of the in-wheel active suspension system and the formulation of the constrained MPC. Section 3 describes the simulation setup, performance evaluation criteria, and statistical metrics used for analysis. Section 4 discusses the simulation results, highlighting the improvements in ride comfort and vibration suppression achieved by the proposed control approach. Finally, Section 5 concludes the paper with key findings, practical implications, and suggestions for future research directions.

2. Vehicle Modelling

To accurately simulate the vehicle's dynamic response, a comprehensive multi-body model was developed. This model captures the essential dynamics of the sprung mass and unsprung mass, which are connected by IW-ASS. The following sections detail the specific mathematical representations and parameters used for each critical component, beginning with the core propulsion system. Following that, the MPC controller will be developed for IW-ASS, enhancing the ride comfort, road holding.

2.1. Active in-wheel model

The integration of IW-ASS represents a major step toward improving ride comfort, road holding, and overall vehicle stability. Unlike conventional suspension systems that rely on passive elements such as springs and dampers, an IW-ASS employs an actuator, often hydraulic, electromagnetic, or electro-hydraulic, that can directly generate control forces to counteract road disturbances. This configuration allows for faster and more accurate force responses, enabling the suspension system to adapt in real-time to changing road conditions and dynamic driving maneuvers. To simplify the model while retaining its physical relevance, the following assumptions are made:

(1) Linearity of suspension components: The suspension spring and damper are assumed to behave linearly within the operating range, although in practice, nonlinearity may arise due to large displacements or hysteresis effects.
(2) Linear tire stiffness: The tire is modeled as a linear spring, neglecting damping and nonlinearities such as tire deflection saturation.
(3) Small displacement approximation: Vertical displacements of the sprung and unsprung masses are assumed to be small relative to the wheelbase, allowing linearization of the governing equations.
(4) Single-wheel isolation: The quarter-car model assumes symmetry, where each wheel behaves independently, ignoring roll and pitch dynamics. This simplifies analysis but can be extended to half- or full-car models for more complex studies.
(5) Actuator response: The active actuator is assumed to generate the commanded force instantaneously and linearly, without delays or saturation, which represents an ideal case. In practical scenarios, actuator dynamics must be considered.

(6) Neglecting frictional losses: Friction in suspension joints and in-wheel motor bearings is neglected to focus solely on vertical dynamics.

The vehicle system under consideration is typically represented by a quarter-car model, which captures the essential vertical dynamics of a single wheel and its associated suspension system. The suspension dynamics are influenced by spring and damping forces, as well as the active actuator force (f_a), which is applied between the sprung and unsprung masses. The tire is modeled as a linear spring (k_w) without damping, consistent with common vehicle dynamics assumptions.

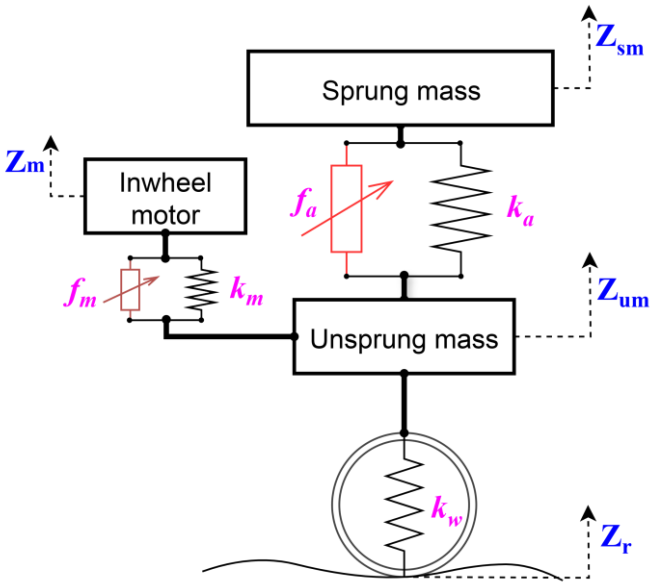

Fig. 1 IW-ASS model

The road disturbance input, denoted as Z_r, excites the system through the tire stiffness. The resulting dynamic response includes the vertical displacements of the sprung mass (Z_{sm}), unsprung mass (Z_{um}), and motor mass (Z_m). As shown in Fig. 1, the system is governed by the following key elements: Suspension stiffness (k_a) and actuator force (f_a) act between the sprung and unsprung masses. Motor suspension stiffness (k_m) and damping (f_m) couple the in-wheel motor to the unsprung mass. Tire stiffness (k_w) connects the unsprung mass to the road profile. The equation can be computed by:

$$m_s\ddot{Z}_{sm} = -k_a\left(Z_{sm} - Z_{um}\right) - c_a\left(\dot{Z}_{sm} - \dot{Z}_{um}\right) - f_a \tag{1}$$

The physical parameters used in the simulation are summarized as follows: the sprung mass, $m_s = 270$kg, the unsprung mass, $m_u = 40$kg, suspension stiffness, $k_a = 22{,}000$N/m, damping coefficient, $c_a = 200$Ns/m, and tire stiffness, $k_w = 220{,}000$N/m. These values are selected based on typical electric vehicle configurations equipped with in-wheel motors, where the increased unsprung mass reflects the additional motor and actuator assembly. All parameters are assumed constant throughout the simulation to maintain model linearity and ensure comparability between the passive and MPC-controlled cases, which can be represented as:

$$m_u\ddot{Z}_{um} = k_a\left(Z_{sm} - Z_{um}\right) + c_a\left(\dot{Z}_{sm} - \dot{Z}_{um}\right) + k_w\left(Z_r - Z_{um}\right) + k_m\left(Z_m - Z_{um}\right) + f_m + f_a \tag{2}$$

$$m_m\ddot{Z}_m = -k_m\left(Z_m - Z_{um}\right) - f_m \tag{3}$$

This three-mass formulation captures the additional dynamics introduced by the in-wheel motor compared to traditional two-mass quarter-car models. In particular, the increased unsprung mass and motor coupling effects significantly affect ride comfort and road-holding ability. Thus, the active actuator is crucial for counteracting hub vibrations and ensuring stability.

2.2. Model predictive controller design

MPC has been adopted in this research owing to its inherent capability to handle multivariable systems, constraints on inputs and outputs, and predictive decision-making over a finite horizon [1]. The central principle of MPC involves solving a finite-horizon optimal control problem at each sampling instant by predicting the future behavior of the vehicle suspension states. The first element of the computed optimal control sequence is applied, while the optimization is repeated at subsequent sampling instants in a receding horizon manner.

2.2.1. Assumptions for MPC formulation

To simplify the controller design while maintaining sufficient accuracy, the following assumptions are made:

(1) Linearized Dynamics: The quarter-car model with electro-hydraulic actuator and electro-servo valve is approximated by a linear discrete-time state-space model around the nominal operating point. Nonlinear valve characteristics are linearized to ensure the tractability of optimization.

(2) Full State Availability: It is assumed that all relevant states of the suspension system, including sprung mass displacement, unsprung mass displacement, and their velocities, are either directly measurable or estimated through an observer (Kalman filter or Luenberger observer).

(3) Constant Parameters within Prediction Horizon: Parameters such as sprung mass m_s, damping coefficient c_a, and suspension stiffness k_a are assumed constant within each prediction horizon, despite possible long-term variations due to road profile or payload.

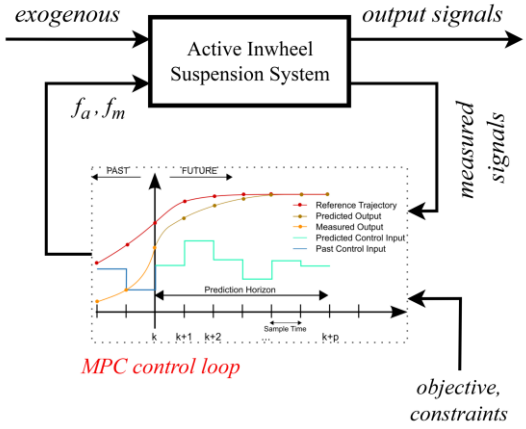

Fig. 2 MPC control schematic for IW-ASS

(4) Limited Control Force: The electro-hydraulic actuator can provide a bounded control force, expressed as:

$$F_{min} \le F(t) \le F_{max} \tag{4}$$

where F_{min} and F_{max} denote the physical actuator limits.

2.2.2. State-space representation for IW-ASS

The continuous-time dynamics of the IW-ASS model can be expressed as:

$$\begin{cases} \dot{x}(t) = A_c x(t) + B_c u(t) + E_c w(t) \\ y(t) = C_c x(t) \end{cases} \tag{5}$$

where $x(t) = \left[Z_{sm}\ \dot{Z}_{sm}\ Z_{um}\ \dot{Z}_{um}\ Z_m\ \dot{Z}_m\right]^T$ is the state vector, $u(t) = F(t)$ is the control force from the actuator; $w(t)$ is the road

disturbance input, *y(t)* represents the measurable outputs such as body acceleration or suspension deflection.

For MPC implementation as displayed in Fig. 2, the IW-ASS model is discretized with a sampling time that can be represented as:

$$\begin{cases} x(k+1) = A_d x(k) + B_d u(k) + E_d w(k) \\ y(k) = C_d x(k) \end{cases} \tag{6}$$

2.2.3. Prediction model and optimization problem

Over a prediction horizon N_p, the future states can be expressed compactly as:

$$X = \Phi x(k) + \Gamma U + \Psi W \tag{7}$$

where $X = \left[x(k+1)\ x(k+2) \ldots x(k+N_p)\right]^T$; $U = [u(k)\ u(k+1) \ldots u(k+N_c-1)]^T$; Φ, Γ, Ψ are prediction matrices derived from A_d, B_d, E_d.

The cost function is defined to balance ride comfort, road holding, and control effort can be calculated by:

$$J = \sum_{i=1}^{N_p} \left(\left\| y(k+i) - r(k+i) \right\|_Q^2 + \left\| \Delta u(k+i-1) \right\|_R^2 \right) \tag{8}$$

where Q penalizes deviation of the vehicle states from desired references (e.g., minimizing body acceleration and suspension deflection); R penalizes excessive control effort to reduce actuator wear, $\Delta u(k) = u(k) - u(k-1)$ represents the change in control force.

2.2.4. Constraints for the MPC controller

The optimization problem is subject to the following constraints:

(1) Actuator Force Limits:

$$F_{min} \le u(k) \le F_{max} \tag{9}$$

(2) Suspension Deflection Constraints:

$$\left| Z_{sm}(k) - Z_{um}(k) \right| \le \delta_{\max} \tag{10}$$

(3) Tire Deflection Constraints:

$$\left| Z_{um}(k) - Z_r(k) \right| \le \delta_{t,\max} \tag{11}$$

The constrained quadratic optimization problem can then be stated as:

$$\begin{aligned} &\min_U J = \frac{1}{2} U^T H U + f^T U \\ &\text{subject o? } GU \le b \end{aligned} \tag{12}$$

where *H* and *f* are derived from prediction matrices and weighting factors, while *G* and *b* encode actuator and suspension constraints.

At each sampling instant, the optimization problem is solved using a quadratic programming (QP) solver [30]. The first control input *u(k)* from the optimal sequence is applied to the suspension actuator, and the horizon is shifted forward, ensuring

adaptability to varying road conditions and uncertainties in vehicle parameters.

The MPC framework utilized in this study is configured with a sampling time of T_s = 1ms, a prediction horizon of (p = 20), and a control horizon of (m = 5). The weighting matrices are defined as (Q = diag[1,0.5,0.2,0.1]) to penalize deviations in the system states, while (R = 0.05) is applied to regulate control effort. The actuator force constraints are specified as (F_{min} = -2000N) and (F_{max} = 2000N), consistent with the operational range of a typical electro-hydraulic actuator integrated within an in-wheel suspension module. These parameters were systematically tuned to achieve an optimal trade-off between vibration attenuation and actuator energy efficiency within practical operating limits.

All simulations and optimization procedures were conducted in MATLAB/Simulink R2023a. The discrete-time state-space model of the IW-ASS system was derived using the *c2d* function with a zero-order hold (ZOH) discretization scheme. At each sampling instant, the constrained quadratic optimization problem (Eq. (12)) was solved using MATLAB's *quadprog* solver from the Optimization Toolbox, ensuring real-time computational efficiency. The simulation time step was maintained at 1 ms, and the numerical convergence of the MPC algorithm was validated across multiple prediction and control horizon configurations.

3. Generalization and Number Synthesis

This section provides a generalized numerical evaluation of the proposed control system by analyzing the simulation signals under different operational scenarios. The assessment focuses on two key statistical measures: the maximum absolute values and the Root Mean Square (RMS) values. These indices serve as quantitative indicators of suspension performance in terms of peak disturbance attenuation and overall vibration energy, respectively. By synthesizing the numerical results, a comprehensive understanding of controller effectiveness is achieved, enabling objective comparisons across different control configurations.

3.1. Evaluating maximum absolute values

The maximum absolute value is an important performance indicator, reflecting the system's ability to suppress extreme responses in dynamic conditions. For each signal under consideration, the maximum magnitude is computed as:

$$x_{\max} = \max\left(|x(t)|\right), \quad t \in [0, T] \tag{13}$$

where *x(t)* represents the time-domain signal of interest, and T denotes the simulation horizon. This metric is particularly relevant for critical parameters such as suspension deflection, tire dynamic load, and vehicle body acceleration.

Fig. 3 collectively demonstrates the effectiveness of the proposed MPC-based active suspension system in mitigating extreme system responses compared to a passive suspension. In the first figure, the maximum displacement of the sprung mass is consistently lower with MPC control across different prediction horizons *p* and control horizons *m*, indicating superior suppression of large body oscillations and improved ride comfort. The second figure, which evaluates the unsprung mass dynamics, shows that passive suspension leads to higher peak fluctuations in wheel movement, whereas the MPC controller substantially reduces these variations, particularly at larger prediction horizons, thereby enhancing road-holding capability. Finally, the third figure highlights maximum tire deflections, where the MPC-controlled system achieves significantly smaller peaks than the passive counterpart, ensuring continuous tire–road contact and improved vehicle stability. Taken together, these results confirm that MPC outperforms passive suspension in minimizing extreme responses, offering simultaneous improvements in ride comfort, road holding, and overall safety.

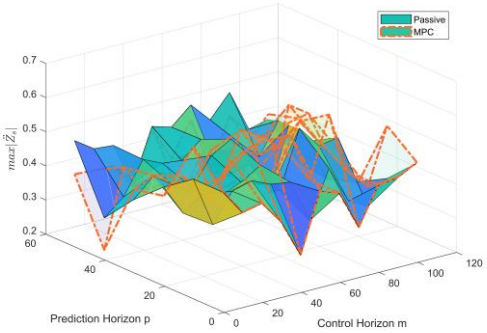

(a) Maximum absolute values of the sprung mass acceleration

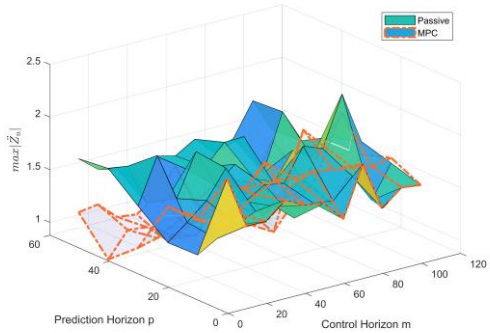

(b) Maximum absolute values of the unsprung mass acceleration

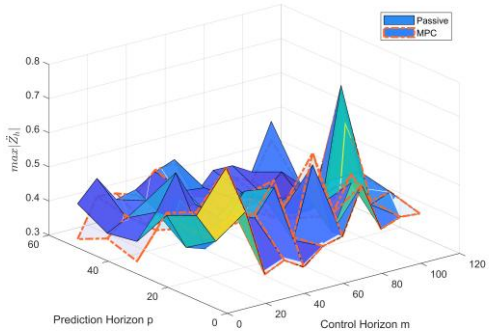

(c) Maximum absolute values of the in-wheel motor acceleration

Fig. 3 Maximum absolute values of the sprung mass, unsprung mass, and in-wheel motor accelerations

3.2. Evaluating the RMS values

While the maximum absolute value highlights instantaneous peaks, the RMS value provides an overall measure of signal energy and long-term vibration intensity. It is calculated as:

$$x_{RMS} = \sqrt{\frac{1}{T}\int_0^T \left(x(t)\right)^2 dt} \tag{14}$$

Fig. 4(a), the RMS values vary between approximately 0.1 and 0.4. It is evident that the MPC surfaces generally remain lower than the Passive surfaces, indicating that MPC achieves reduced variability in system response under most prediction and control horizon configurations. This reflects that MPC contributes to better performance in terms of stability, especially at moderate values of prediction and control horizons, where fluctuations are visibly dampened compared to the Passive system.

Fig. 4(b) shows a different range of results, with RMS values spanning from about 0.3 to 0.7. Here, the Passive control tends to lie above the MPC, suggesting higher variability under the Passive case. MPC again demonstrates its ability to reduce fluctuations, maintaining RMS values in a narrower band. This highlights the robustness of MPC in handling dynamic changes more effectively, where increasing prediction and control horizons help further mitigate variability compared to Passive control.

Fig. 4(c) represents a narrower range of variability, with RMS values roughly between 0.12 and 0.17. The results show a consistent trend where MPC exhibits marginally lower or comparable RMS values compared to Passive control. Although the difference between the two strategies is not as pronounced as in the first two figures, MPC still shows an advantage in reducing oscillations. This suggests that even in cases where system variability is inherently small, MPC can provide additional stability benefits.

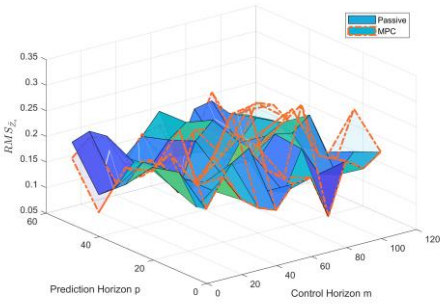

(a) RMS of the sprung mass acceleration

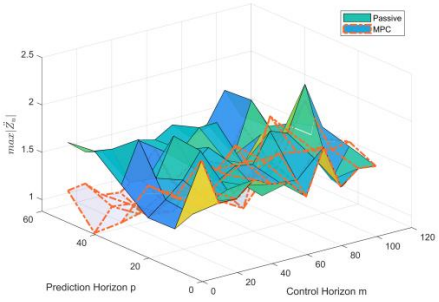

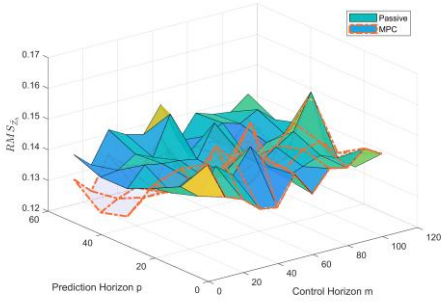

(b) RMS of the unsprung mass acceleration (c) RMS of the in-wheel motor acceleration

Fig. 4 RMS of the sprung mass, unsprung mass, and in-wheel motor accelerations

4. Simulation analysis

To evaluate the performance of the proposed control strategy, the IW-ASS model was subjected to a stochastic road excitation generated in accordance with ISO 8608:2016. Specifically, a Class B road profile was synthesized at a reference spatial frequency n_o=1m^{-1} with a waviness exponent w = 2 and a midpoint roughness coefficient $G_q(n_o) = 64\times10^{-6}m^3$. The time-domain road displacement input was obtained by harmonic superposition with random phase assignment, ensuring statistical consistency with the target power spectral density. A constant vehicle speed of 60 km/h was assumed to convert the spatial frequency domain into the temporal domain, with the generated Class B road roughness profile (Fig. 5) serving as the primary disturbance input for the simulation.

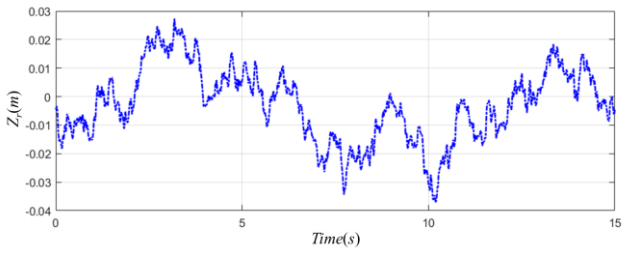

Fig. 5 ISO 8608-2016 class B road exogenous at 60 km/h

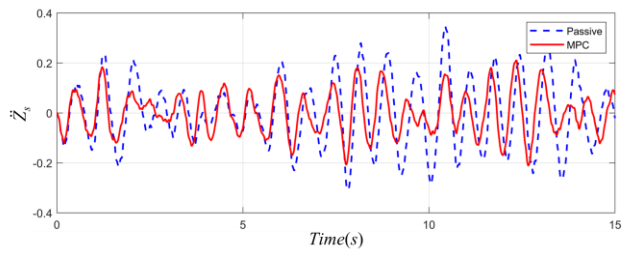

Fig. 6 Acceleration of sprung mass in ISO8608-2016 class B at 60 km/h

Fig. 6 illustrates the time response of the sprung mass acceleration when the vehicle traverses an ISO 8608:2016 Class B road profile at a constant velocity of 60 km/h. The passive suspension system exhibits large oscillations with peak accelerations reaching approximately ±0.3 m/s², which reflect significant ride discomfort and poor vibration isolation. In contrast, the proposed MPC strategy effectively attenuates both the amplitude and frequency of oscillations, thereby reducing the overall acceleration level experienced by the sprung mass. This improvement highlights the controller's capability to mitigate road-induced vibrations and enhance ride comfort under realistic road excitations.

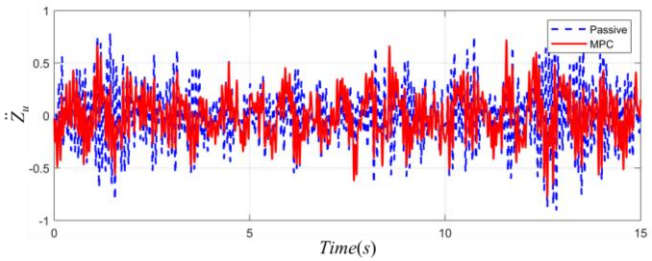

Fig. 7 Acceleration of unsprung mass in ISO8608-2016 class B at 60 km/h

The unsprung mass acceleration response under Class B road excitation at 60 km/h is depicted in Fig. 7. Compared with the passive suspension, the MPC strategy results in noticeable attenuation of high-frequency vibration components while maintaining similar low-frequency dynamics. Although the magnitude of peak accelerations remains within ±1 m/s² for both cases, MPC exhibits reduced fluctuation intensity and smoother transient behavior, which is beneficial for limiting tire–road contact force variations. This outcome demonstrates that MPC not only improves ride comfort by reducing sprung mass accelerations (as shown previously) but also contributes to better road holding and handling stability through improved unsprung mass dynamics.

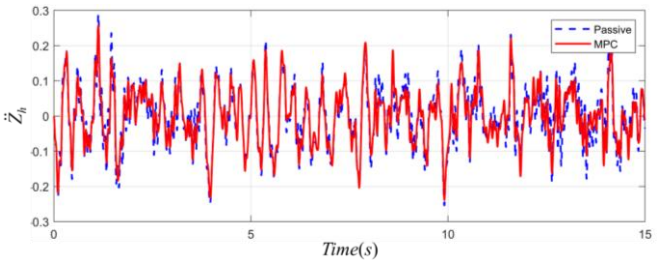

Fig. 8 Acceleration of the hub in ISO8608-2016 class B at 60 km/h

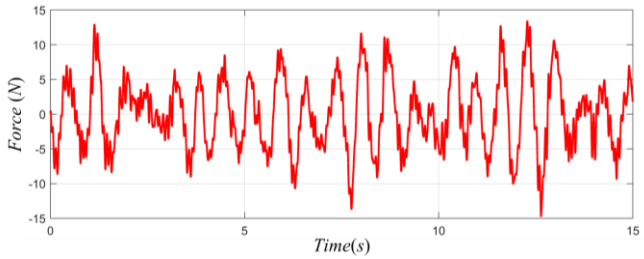

Fig. 9 Controlled forces demand for IW-ASS model

Fig. 8 illustrates the hub acceleration response when the vehicle runs on an ISO 8608:2016 Class B road profile at 60 km/h. Due to the direct influence of the tire–road interaction, both passive and MPC-controlled suspensions exhibit similar oscillation patterns. Nevertheless, the MPC approach achieves a slight reduction in the vibration intensity. Specifically, the RMS value decreases from 0.0859 m/s² (Passive) to 0.0807 m/s² (MPC), corresponding to a reduction ratio of 6.02%. Although the improvement is less pronounced compared to the reductions in sprung mass acceleration (36.44%) and unsprung mass acceleration (18.71%), this attenuation still provides significant benefits by mitigating tire load fluctuations and promoting more stable tire–road contact, while maintaining the controlled force demand of the IW-ASS actuators within the controller's prescribed constraints, as illustrated in Fig. 9. Thus, the MPC controller contributes to improved ride comfort while simultaneously enhancing handling stability.

5. Conclusions

This study proposed a constrained MPC strategy to enhance the dynamic performance of a quarter-car IW-ASS subjected to ISO 8608:2016 Class B stochastic road excitation at a constant speed of 60 km/h. The primary objective is to evaluate the effectiveness of constrained MPC in improving ride comfort, vibration isolation, and road-holding performance compared to a conventional passive suspension. The simulation framework incorporated a high-fidelity vehicle model and predictive optimization to ensure a realistic assessment under standardized operating conditions. The key findings of this study are summarized as follows:

(1) The constrained MPC controller significantly outperformed the passive suspension benchmark, achieving a 36.44% reduction in sprung mass RMS acceleration, which directly translates to improved ride comfort.
(2) The controller achieved an 18.71% reduction in unsprung mass RMS acceleration, indicating enhanced vibration isolation and improved suspension compliance under stochastic disturbances.
(3) A 6.02% reduction in hub acceleration was observed, contributing to more stable tire–road contact and improved road-holding performance.
(4) The MPC formulation successfully enforced actuator and suspension deflection constraints throughout the optimization process, demonstrating the practical feasibility of predictive constraint handling in IW-ASS control design.
(5) The simulation-based analysis provided a quantitative performance benchmark for constrained MPC under standardized road conditions, establishing its capability as a viable control strategy for future IW-ASS applications.

The study highlights the importance of constraint-aware control design in real-world suspension systems, where actuator limits and safety considerations are inherent. Achieving real-time implementation will require careful attention to actuator dynamics, computationally efficient QP solvers, and reliable sensing and estimation pipelines. Future research will extend this work to half- and full-vehicle configurations, supported by hardware-in-the-loop and experimental validation to further evaluate trade-offs among ride comfort, energy consumption, and actuator effort.

Acknowledgments

The author would like to express sincere gratitude to the colleagues at the Faculty of Mechanical – Automotive and Civil Engineering, Electric Power University, and the members of the ITV research team for their valuable support, constructive discussions, and encouragement throughout the course of this research.

Conflicts of Interest

The authors declare no conflict of interest.

References

[1] R. R. Das and E. V. Kumar, “Active Suspension with Model Predictive Control,” International Journal of Engineering and Advanced Technology, vol. 8, no. 6, pp. 2826-2831, 2019.
[2] C. Xing, Y. Zhu, and H. Wu, “Electromechanical Coupling Braking Control Strategy Considering Vertical Vibration Suppression for Vehicles Driven by In-Wheel Motors,” IEEE/ASME Transactions on Mechatronics, vol. 27, no. 6, pp. 5701-5711, 2022.
[3] A. Swief, A. El-Zawawi, and M. El-Habrouk, “A Survey of Model Predictive Control Development in Automotive Industries,” Proceedings of 2019 International Conference on Applied Automation and Industrial Diagnostics (ICAAID), pp. 1-7, 2019.
[4] D. T. Tu, “Enhancing Road Holding and Vehicle Comfort for an Active Suspension System Utilizing Model Predictive Control and Deep Learning,” Engineering, Technology & Applied Science Research, vol. 14, no. 1, pp. 12931-12936, 2024.
[5] Z. Zhao, L. Gu, J. Wu, X. Zhang, and H. Yang, “An Integrated Vibration Elimination System with Mechanical-Electrical-Magnetic Coupling Effects for In-Wheel-Motor-Driven Electric Vehicles,” Electronics, vol. 12, no. 5, 2023.
[6] H. Jiang, C. Wang, Z. Li, and C. Liu, “Hybrid Model Predictive Control of Semiactive Suspension in Electric Vehicle with Hub-Motor,” Applied Sciences, vol. 11, no. 1, article no. 382, 2021.

[7] Z. Yueying, Y. Chuantian, Y. Yuan, W. Weiyan, and Z. Chengwen, "Design and Optimisation of an In-Wheel Switched Reluctance Motor for Electric Vehicles," IET Intelligent Transport Systems, vol. 13, no. 1, pp. 175-182, 2019.
[8] Z. Zhao, H. Taghavifar, H. Du, Y. Qin, M. Dong, and L. Gu, "In-Wheel Motor Vibration Control for Distributed-Driven Electric Vehicles: A Review," IEEE Transactions on Transportation Electrification, vol. 7, no. 4, pp. 2864-2880, 2021.
[9] Y. Qin, Z. Wang, K. Yuan, and Y. Zhang, "Comprehensive Analysis and Optimization of Dynamic Vibration-Absorbing Structures for Electric Vehicles Driven by In-Wheel Motors," Automotive Innovation, vol. 2, pp. 254-262, 2019.
[10] K. Deepak, M. A. Frikha, Y. Benômar, M. El Baghdadi, and O. Hegazy, "In-Wheel Motor Drive Systems for Electric Vehicles: State of the Art, Challenges, and Future Trends," Energies, vol. 16, no. 7, pp. 1-31, 2023.
[11] H. Xu, J. Liu, T. Luo, Y. Yao, and C. Lv, "Model-Based Design of an Active Suspension for the Improvement of In-Wheel Motor Drive Electric Vehicle," IEEE Access, vol. 12, pp. 45597-45615, 2024.
[12] Z. Zhao, L. Zhang, J. Wu, L. Gu, and S. Li, "Vertical-Longitudinal Coupling Effect Investigation and System Optimization for a Suspension-In-Wheel-Motor System in Electric Vehicle Applications," Sustainability, vol. 15, no. 5, article no. 4168, 2023.
[13] Y. Qin, C. He, X. Shao, H. Du, C. Xiang, and M. Dong, "Vibration Mitigation for In-Wheel Switched Reluctance Motor Driven Electric Vehicle with Dynamic Vibration Absorbing Structures," Journal of Sound and Vibration, vol. 419, pp. 249-267, 2018.
[14] Y. Zhu, C. Zhao, J. Zhang, and Z. Gong, "Vibration Control for Electric Vehicles with In-Wheel Switched Reluctance Motor Drive System," IEEE Access, vol. 8, pp. 7205-7216, 2020.
[15] Y. Qin, C. He, P. Ding, M. Dong, and Y. Huang, "Suspension Hybrid Control for In-Wheel Motor Driven Electric Vehicle with Dynamic Vibration Absorbing Structures," IFAC-PapersOnLine, vol. 51, no. 31, pp. 973-978, 2018.
[16] R. He and J. C. Wang, "Vertical Vibration Control of an In-Wheel Motor-Driven Electric Vehicle Using an In-Wheel Active Vibration System," Asian Journal of Control, vol. 22, no. 2, pp. 879-896, 2020.
[17] N. J. Wills, Y. Y. Li, J. Z. Jiang, T. L. Hill, S. A. Neild, and M. Dhaens, "Using Inerter-Integrated Absorbers to Improve the Performance of an In-Wheel Motor System," Vehicle System Dynamics, vol. 62, no. 8, pp. 2162-2183, 2024.
[18] Y. Qin, Z. Zhao, Z. Wang, and G. Li, "Study of Longitudinal–Vertical Dynamics for In-Wheel Motor-Driven Electric Vehicles," Automotive Innovation, vol. 4, pp. 227-237, 2021.
[19] B. Xu, C. Xiang, Y. Qin, P. Ding, and M. Dong, "Semi-Active Vibration Control for in-Wheel Switched Reluctance Motor Driven Electric Vehicle with Dynamic Vibration Absorbing Structures: Concept and Validation," IEEE Access, vol. 6, pp. 60274-60285, 2018.
[20] G. Long, F. Ding, N. Zhang, J. Zhang, and A. Qin, "Regenerative Active Suspension System with Residual Energy for In-Wheel Motor Driven Electric Vehicle," Applied Energy, vol. 260, article no. 114180, 2020.
[21] Y. Chen, S. Chen, Y. Zhao, Z. Gao, and C. Li, "Optimized Handling Stability Control Strategy for a Four In-Wheel Motor Independent-Drive Electric Vehicle," IEEE Access, vol. 7, pp. 17017-17032, 2019.
[22] M. Liu, Y. Zhang, J. Huang, and C. Zhang, "Optimization Control for Dynamic Vibration Absorbers and Active Suspensions of In-Wheel-Motor-Driven Electric Vehicles," Proceedings of the Institution of Mechanical Engineers, Part D: Journal of Automobile Engineering, vol. 234, no. 9, pp. 2377-2392, 2020.
[23] Q. Li, Z. Chen, H. Song, and Y. Dong, "Model Predictive Control for Speed-Dependent Active Suspension System with Road Preview Information," Sensors, vol. 24, no. 7, article no. 2255, 2024.
[24] Z. Deng, X. Li, X. Li, S. Zhao, and H. Wei, "Mechanism Analysis and Optimum Control of Negative Airgap Eccentricity Effect for In-Wheel Switched Reluctance Motor Driving System," Nonlinear Dynamics, vol. 111, pp. 9075-9093, 2023.
[25] A. Rezig, W. Boudendouna, A. Djerdir, and A. N'Diaye, "Investigation of Optimal Control for Vibration and Noise Reduction In-Wheel Switched Reluctance Motor Used in Electric Vehicle," Mathematics and Computers in Simulation, vol. 167, pp. 267-280, 2020.
[26] J. Zhao, J. Dong, P. K. Wong, X. Ma, Y. Wang, and C. Lv, "Interval Fuzzy Robust Non-Fragile Finite Frequency Control for Active Suspension of In-Wheel Motor Driven Electric Vehicles with Time Delay," Journal of the Franklin Institute, vol. 359, no. 12, pp. 5960-5990, 2022.
[27] T. Huang, H. Pan, W. Sun, and H. Gao, "Sine Resistance Network-Based Motion Planning Approach for Autonomous Electric Vehicles in Dynamic Environments," IEEE Transactions on Transportation Electrification, vol. 8, no. 2, pp. 2862-2873, 2022.
[28] M. Bai and W. Sun, "Disturbance-Resilient Model Predictive Control for Active Suspension Systems with Perception Errors in Road Preview Information," Journal of the Franklin Institute, vol. 362, no. 15, article no. 107957, 2025.
[29] T. Huang, J. Wang, and H. Pan, "Approximation-Free Prespecified Time Bionic Reliable Control for Vehicle Suspension," IEEE Transactions on Automation Science and Engineering, vol. 21, no. 4, pp. 5333-5343, 2024.
[30] D. Q. Mayne, J. B. Rawlings, C. V. Rao, and P. O. M. Scokaert, "Constrained Model Predictive Control: Stability and Optimality," Automatica, vol. 36, no. 6, pp. 789-814, 2000.